Proceedings of ICFA Mini-Workshop on Tracking for Collimation in Particle Accelerators, CERN, Geneva, Switzerland, 30 October 2015, CERN Yellow Reports: Conference Proceedings, Vol. 2/2018, CERN-2018-011-CP (CERN, Geneva, 2018)

Updated implementation of collimator materials in SixTrack and MERLIN codes*

E. Quaranta†, A. Valloni, R. Bruce, A. Mereghetti, S. Redaelli
CERN, 1211 Geneva, Switzerland.

Abstract
The High-Luminosity upgrade of the Large Hadron Collider will push various operational parameters of the machine beyond the design values. The LHC beam collimation system turns out to be one of the bottlenecks for the achievement of the future challenging beam parameters. In particular, various limitations have been identified that call for an improvement of the materials used in various collimator types. An R&D program at CERN explores novel composite materials for collimators with improved mechanical robustness and reduced electromagnetic impedance that can address the main limitations of the present system. A new collimator material implementation introduced in SixTrack and MERLIN, simulation codes for beam collimation at the LHC, allows to simulate advanced collimators based on novel composite materials. An immediate application of this novelty in the two codes is to study the effect of the upgrades collimators on the cleaning performance of the collimation system. After presenting the methods used to model composite materials in each code, we apply it to the case of cleaning simulations with novel collimator materials in the LHC, where the results obtained with SixTrack and MERLIN are compared.

Keywords
SixTrack, MERLIN, composite materials, collimation, cleaning.

1 Introduction

The collimation system at the Large Hadron Collider (LHC) is designed to efficiently absorb high energy beam losses and ensure machine protection [1, 2]. Since the first design of the present system [2], non-metallic primary and secondary collimators (TCPs and TCSGs, respectively) turn to provide the largest contribution to the electromagnetic impedance of the whole machine [3]. The impedance is an electromagnetic concern of paramount importance that may obstacle the achievement of the High Luminosity (HL) upgrade of the LHC [4], which aims at smaller beam emittance and doubled beam current. The small collimator gaps required to achieve the design beam performance, as well as the low electrical conductivity of the carbon-fiber-carbon (CFC) composite used for the collimator jaws contribute to the large impedance of secondary collimators.

In order to reduce beam instability in operation caused by the impedance, an R&D program has started at CERN to explore novel composite materials that can replace the present CFC and match the HL-LHC requirements. The developed materials combine the excellent thermal properties of graphite or diamond with those of metals and metal-based ceramics of high mechanical strength and, above all, good electrical conductivity. A number of possible composites have been narrowed down to molybdenum-carbide-graphite (MoGr) and copper-diamond (CuCD) [5], which so far are the most promising candidates for the new generation of advanced collimators.

*Research supported by the High Luminosity LHC project and EuCARD-2 (Grant agreement 312453).
†Politecnico di Milano, Piazza Leonardo da Vinci 32, 20133 Milan, Italy.

https://doi.org/10.23732/CYRCP-2018-002.109.

Material properties are measured through rigorous experimental testing [6]. Then, numerical simulations use the observed properties to investigate the effect of different collimator materials on the cleaning performance of the LHC collimation system. The implementation of new composite materials has been introduced in the existing SixTrack and MERLIN codes, which are the tools routinely used for beam cleaning studies in large circular machines, such as the LHC.

SixTrack [7–9] is a tracking code, written in Fortran 77, and used for simulating longitudinal and transverse dynamics of single beam particles in ultra-relativistic accelerators. The code was extended [10] to evaluate the performance of a collimation system in terms of induced loss pattern and cleaning performance. This setup became the standard tool for collimation studies at CERN. The dynamics of a large number of protons that populate the beam halo can be studied throughout the simulated ring, which is accurately described by a detailed aperture model of the LHC. The interactions of the particles with the collimator materials, which generates different scattering mechanisms with either the atomic shells or the nuclei of the material, are also simulated. In SixTrack, scattering mechanisms are modelled by a Monte-Carlo code that has been recently reviewed and improved [11].

MERLIN [12] is an accelerator physics library originally written in the years 2000 for specific studies on the International Linear Collider [13]. Later, it was decided to update the MERLIN library to include the requirements for complementary simulations of the LHC collimation system. MERLIN is written in C++, which makes it a modular tool and therefore easy to modify. It offers thick lens tracking, an on-line aperture check, and a number of physics processes. The scattering physics in MERLIN has recently been updated [14].

Both SixTrack and MERLIN codes build composite materials for collimator in similar way, but differ in the approach to perform point-like scattering in the composites. In this work, the implementation methods used in the two codes are described and results of the scattering physics for composite materials are compared. Tracking simulations performed with SixTrack and MERLIN are then discussed, for the case of nominal LHC and 7 TeV proton beams, to assess the collimation efficiency when advanced collimators are deployed in the system.

1.1 Mechanisms of particle-matter interaction

Before going into the details of the material implementations adopted in the codes, it can be useful to recall the main scattering processes that a proton can undergo when interacts with matter. SixTrack and MERLIN allow to simulate a set of proton-matter interactions in the collimator jaw, which are classified in:

- *Continous interactions*, i.e. ionization, multiple Coulomb scattering and Rutherford scattering.
- *Point-like nuclear interactions*, i.e. nuclear elastic, inelastic and inelastic-diffractive scattering.

1.1.1 Ionization

When a charged particle collides against the atomic electrons along the path of the traversed material, the energy transferred from the incoming particle to the electrons can be high enough to put them in motion, and then ionising the material. The energy loss along the path, commonly called stopping power, is expressed by the Bethe-Bloch equation [15]:

$$-\frac{dE}{dx} = Kz^2\frac{Z}{A}\frac{1}{\beta_{rel}^2}\left[\frac{1}{2}\ln\frac{2m_e c^2\beta_{rel}^2\gamma^2 T_{max}}{I^2} - \beta_{rel}^2 - \frac{\delta}{2}\right] \tag{1}$$

where Z and A are respectively the atomic number and the atomic mass of the material, m_e is the electron mass while z, β_{rel}^2 and γ are respectively the charge, the velocity and the relativistic factor of the incident particle. I is the mean excitation energy, T_{max} is the maximum kinetic energy that an electron can gain in one single collision and finally δ is a correction term depending on the density of the material. K/A is

a constant, equal to $(4\pi N_A r_e^2 m_e c^2)/A = 0.307075$ MeV g^{-1} cm^2 for $A = 1$ g mol^{-1}. The energy loss per unit length (in MeV g^{-1} cm^2) given as a function of the particle energy in any material varies very slowly for $E >$100 TeV [16]. In SixTrack, dE/dx at the reference energy of 450 GeV/c was initially used to estimate the energy lost by ionization in both the injection and the top energy case. However, to more accurately estimate dE/dx, the revised version of the scattering routine [11] now computes Eq. 1 for protons of any given energy. This calculation requires information on atomic parameters, such as Z, A, I, as well as on the material density, needed for the conversion to metric units (GeV/m).

1.1.2 Multiple Coulomb Scattering (MCS)

When a charged particle traverses a medium, it faces many small angle deflections, most of them caused by Coulomb scattering from the nuclei, so the origin of its name. According to Moliere's theory [17], the rms of the deflection angle θ after crossing a thickness s of material is given by:

$$\theta(s) = \frac{13.6MeV}{\beta_{rel}cp} z \sqrt{\frac{s}{X_0}} \left[1 + 0.038 \ln(\frac{s}{X_0})\right] \tag{2}$$

where p is the momentum of the incident particle. X_0 is the radiation length of the material and indicates the mean length of the medium that the particle has to traversed to reduce its energy by $1/e$.

1.1.3 Rutherford scattering

This mechanism takes place when the incoming proton passes very close to a nucleus and is deflected away with a large scattering angle by the repulsive force due to the positive charge of the nucleus. It is still considered as Coulomb scattering, but with a finite cross section defined as:

$$\frac{d\sigma_{ruth}}{dt} = 4\pi\alpha^2(\hbar c)^2 \left(\frac{Z}{t}\right)^2 e^{-0.856\times10^3 tR^2} \tag{3}$$

where $a = 1/137$, $(\hbar c)^2 = 0.389$ GeV^{2}mbarn and Z is the atomic number. The factor proportional to $1/t^2$ is the classical Rutherford formula for Coulomb scattering near a point charge. The exponential term is the nuclear form factor that accounts for the finite size of the nucleus. R is the radius of the nucleus that, if not measured, is calculated by $R = 2\hbar c\sqrt{b}$. b is the slope factor of the angular distribution for proton-nucleus elastic interaction, which is correlated to the mass number of the material by the formula $b = 14.1A^{2/3}$.

1.1.4 Point-like interactions

Unlike the previous mechanisms that occur over a certain length of the material, proton-matter interaction can also involve an incoming proton and one of the components of the atomic structure of the traversed material (like nucleons, i.e. protons or neutrons, or the entire nucleus). The proton-nucleon interactions can be elastic, inelastic or inelastic-diffractive.

In *nuclear elastic* scattering, the beam particle survives to the event it underwent, changing direction and energy according to the two-body kinematics. With a look at the LHC, nuclear elastic scattering, together with ionisation and MCS, plays a major role in diluting the beam particles and reducing their energy when they survive to the impact onto a collimator.

In *nuclear inelastic* scattering the incoming particle do not come out from the material (and therefore considered lost there), and generate new (secondary) particles. These events are extremely important in the design of beam intercepting devices, as they provide an estimation of the beam attenuation.

Moreover, *single-diffractive* (SD) scattering also exists. The momentum transferred during the collision can excite a nucleon of the medium, that have enough energy to travel some distance through the medium. However, the probability that the incoming proton survives without being lost is null.

From here the reason why SD scattering is considered a quasi-elastic mechanism. This process is very important for LHC collimation because part of the betatron halo is converted into an off-momentum halo, due to the larger variation in energy of the particles after the event.

1.1.5 Particle mean free path

The *mean free path* is the length before a point-like interaction or a Rutherford scattering event occurs between the incoming particle and the atoms of the medium travelled. The mean free path λ_i of each process i can be expressed in terms of the cross section of the interaction with the atoms of the medium through the formula [18]:

$$\lambda_i = \frac{1}{\sigma_i} \frac{A}{\rho N_A} \tag{4}$$

where σ_i is the cross section of the process, ρ and A are respectively the material density and the atomic weight, and N_A is the Avogadro number. A *total collision length* is also defined as:

$$\frac{1}{\lambda_{tot}} = \sigma_{tot} = \sigma_{el} + \sigma_{SD} + \sigma_{inel} + \sigma_{ruth} \tag{5}$$

that takes into account all the possible elastic, quasi-elastic and inelastic collisions, as well as the Rutherford scattering events, that can occur along the path. In the LHC, the *inelastic collision length* λ_{inel} is particularly important for the collimator design, as it expresses the average length needed to achieve an attenuation of $1/e$ of the primary particle, by nuclear inelastic events.

2 Implementation of new materials in SixTrack

A dedicated database embedded in SixTrack, called SCDATA, stores the material properties required by the scattering routine to simulate the different scattering processes. Some of the input parameters are:

- Atomic and mass number,
- Material density,
- Radiation length,
- Mean excitation energy,
- Cross sections of the point-like interactions,
- Rutherford scattering cross section.

So far, only pure materials were implemented in the code: aluminium, beryllium, carbon, copper, lead, and tungsten. The values of the material properties were directly taken from Ref. [16] and used in the formulas discussed below to calculate the parameters required by the code, such as cross sections and nuclear interaction lengths.

Composite materials, some already used in the present LHC collimators and some being considered for the HL-LHC collimation upgrades, have been added to the existing database. The newly implemented materials are:

- Molybdenum-Graphite composite (MoGr, grade MG-6530Aa),
- Copper-Diamond composite (CuCD),
- Tungsten Heavy Alloy Inermet-180 (IT-180),
- Glidcop.

The material routine in SixTrack treats mono-element materials. In the presented approximation, composite materials are dealt with by calculating off-line the input parameters required by the code, starting from the material composition. The result is a“composit” nucleus weighted on the constituent

nuclei. The approximation considers an "averaged" composite material, therefore not described at the atomic level.

Here we discuss how the values of each parameter required by the SixTrack material database are obtained for composite materials. The atomic number Z and atomic weight A of each compound material was calculated as average weighted on the atomic fraction of their components i:

$$p = \sum_i at_i \cdot p_i, \quad \text{(i = 1, 2,...)} \tag{6}$$

where p is the property of the compound to be computed, p_i are the values of the property, extracted from the Particle Data Group database [16], for the i-th element present in the material and at_i the atomic content of each element in the composite.

The mean ionization energy I and the radiation length χ_0 must be provided to SixTrack to calculate the energy lost by ionization and correctly simulate the MCS events. According to [16], for a composite material, these parameters can be approximated by:

$$\frac{1}{p} = \sum_i \frac{wt_i}{p_i}, \tag{7}$$

where wt_i is the mass fraction of the i-th element in the compound. Once more, p_i refer to values in [16].

The incoming protons can interact with the nuclei of the material in different ways. Each process is characterized by its cross section (σ), that gives the probability for the scattering process to occur in a specific material. The total nuclear cross section (σ_{tot}) and the nuclear inelastic cross sections (σ_{inel}) at 450 GeV were implemented in SixTrack, calculated as follows:

$$\sigma = \frac{A}{N_A \rho \lambda}, \tag{8}$$

with N_A Avogadro's number, A and ρ the average atomic weight and the density of the material, respectively. For composite materials, the collision length (λ_{tot}) and the inelastic length (λ_{inel}) are calculated as in Eq. (7). The Rutherford scattering cross section σ_{ruth} was derived through Eq. 3. In particular, the radius R and the slope factor b were computed by using the average mass weight for the "composite" nucleus, calculated as in Eq. 6.

Table 1 lists the most important parameters, along with the atomic composition, of the materials considered in the implementation. The properties of CFC are also reported in the table for comparison, although the material was already coded in SixTrack as pure carbon.

Table 1: Summary of the properties of the new composite materials added in SixTrack: average atomic number Z, average atomic weight A, density ρ, electrical conductivity σ_{el}, composition by atomic fractions, radiation length χ_0, collision length λ_{tot} and inelastic scattering length λ_{inel} for 200 GeV/c protons.

	Z	A (g/mol)	ρ (g/cm^3)	σ_{el} (MS/m)	**at. content** (%)	χ_0 (cm)	λ_{tot} (cm)	λ_{inel} (cm)
CFC	6	12.01	1.67	0.14	100 C	25.57	35.45	51.38
MoGR	6.65	13.53	2.50	1	2.7 Mo_2C, 97.3 C	11.93	24.84	36.42
CuCD	11.90	25.24	5.40	12.6	25.7 Cu, 73.3 CD, 1 B	3.16	13.56	20.97
Glidcop	28.82	63.15	8.93	53.8	99.1 Cu, 0.9 Al_2O_3	1.44	9.42	15.36
IT-180	67.66	166.68	18	8.6	86.1 W, 9.9 Ni, 4 Cu	0.39	6.03	10.44

This implementation of composite materials in SixTrack is recently become part of the official release of the code [19].

3 Implementation of new materials in MERLIN

In order to model composite materials for advanced collimators in MERLIN, a new COMPOSITEMATERIAL class was created. The COMPOSITEMATERIAL class allows the user to create a composite material from other existing or user defined materials. These constituent materials may be pure elements or other composites and may be added by fractions of mass (m_i) or number (n_i) using the functions *AddMaterialByMassFraction* or *AddMaterialByNumberFraction*. After all constituents have been added, the *Assemble* function calculates all material properties. An example of constructing CuCD using the COMPOSITEMATERIAL constructor, setting functions, and calculation functions is shown in Fig. 1. In order

```
CompositeMaterial* CuCD = new CompositeMaterial();
  CuCD->SetName("CopperCarbonDiamond");
  CuCD->SetSymbol("CuCD");

  CuCD->AddMaterialByMassFraction(CD,0.3489);
  CuCD->AddMaterialByMassFraction(Cu,0.6467);
  CuCD->AddMaterialByMassFraction(B,0.0044);

  CuCD->SetDensity(5400);
  CuCD->SetConductivity(12.6E6);
  CuCD->Assemble();
  CuCD->VerifyMaterial();
```

Fig. 1: Example of constructing CuCD in MERLIN.

to construct a composite materials from the constituent elements, the mass fraction m_i of constituent i in the composite must be known, which is given by:

$$m_i = \frac{n_i A_i}{\sum_i n_i A_i}, \tag{9}$$

where A_i is the constituent atomic mass and n_i is the number fraction of the constituent in the composite. These fractions may be used to define some composite material properties as a weighted average of the constituent properties. For example the mean atomic mass of the homogeneous composite $\bar{A}$ is:

$$\bar{A} = \sum_i n_i \cdot A_i. \tag{10}$$

and the radiation length χ_0 of a compound material is:

$$\frac{1}{\chi_0} = \sum_i \frac{m_i}{\chi_i} \tag{11}$$

where χ_i is the radiation length of the ith element. In order to define the path length for a proton scattering in the composite in MERLIN, *i.e.* the distance traversed before interacting with a nucleus, the sum of the calculated cross sections $\sigma_{pN\ tot}$ is used to find the mean free path:

$$\lambda_{tot} = \frac{\bar{A}}{\sigma_{pN\ tot} \cdot \bar{\rho} N_a}, \tag{12}$$

where N_a is Avogadro's constant and ρ the density.

Cross sections for composite nuclear interactions are generated in MERLIN for the composite (as a homogeneous mixture) in order to calculate the mean free path, but are not used for point-like scattering. Working from the constituent cross sections, Eq. 13 is used to find the reference nuclear cross sections (total, inelastic, elastic, or Rutherford).

$$\sigma_{pN} = \sum_i n_i \sigma_{pN\ i}. \tag{13}$$

These properties are used in the application of bulk scattering in MERLIN, *i.e.* MCS and energy loss via ionisation for a composite material.

4 Comparison of composite material implementation in SixTrack and MERLIN

SixTrack and MERLIN use different approaches to treat point-like interactions between the particles of the incoming beam and the collimator material. In SixTrack (we call it "6T-method"), point-like scattering are performed from an imaginary composite nucleus, which is the weighted average of the constituent nuclei. In MERLIN, when a point-like events occurs, an elementary constituent nucleus of the material is randomly selected and the proton scatters from the constituent nucleus with corresponding cross sections and all other properties. In this paper, we refer to this approach as "MERLIN-method". However, MERLIN can also reproduce a similar approach to that of SixTrack by enabling point-like scattering from the composite nucleus instead of the constituent nuclei. We call the latter "MERLIN-6T method". The different approaches have been compared in order to quantify the errors [20].

To better study the effect on the scattering physics of the different approaches used in the two codes on the scattering physics, a test case was defined. It consists a pencil beam of 6.4×10^6 protons impacting upon 1 cm long block of material. Simulations have been performed in MERLIN and SixTrack, and the results are shown in Fig. 2, 3, 4. In each plot, the red curve represents simulations performed in MERLIN using the "MERLIN-method", the blue curve the "MERLIN-6T-method" and the green curve the results obtained from SixTrack. Fig. 2 shows the change in polar angle θ and particle momentum dp for particles that undergo single diffractive (SD) events in the material block (either MoGr or CuCD). The "MERLIN-method" results in a smaller cross section than SixTrack. It is also the case that the momentum transfer is smaller in SixTrack. The distribution of θ and the spread in energy loss are larger in MERLIN, while SD events resulting in small energy loss are more frequent in SixTrack. Differences between the "MERLIN-method" and "MERLIN-6T-method" are not evident in these plots. The angular and momentum spread for particles that do not undergo point like scattering events are compared in Fig. 3: the trends appear identical. MERLIN and SixTrack provide very similar results, which is expected as for MCS and ionisation the method used for composites is the same in both codes. A comparison of the distributions for total elastic scattering, as simulated by the two codes, is shown in Fig. 4, for MoGr and CuCD: no relevant discrepances between the results are found.

The comparison of the simulated distribution of point-like interactions have shown only small differences between SixTrack and MERLIN, in spite of the different approaches of the two codes in treating composite materials. For the purpose of beam dynamics studies for LHC collimators, we consider these differences small enough. We remind, indeed, that collimators are bulk devices, whose final properties are averaged over the full size of the collimator (several centimetres). Therefore, we are confident that the approximation done in the "SixTrack-method" are consistent and can reproduce the properties of composite materials for collimators without large errors.

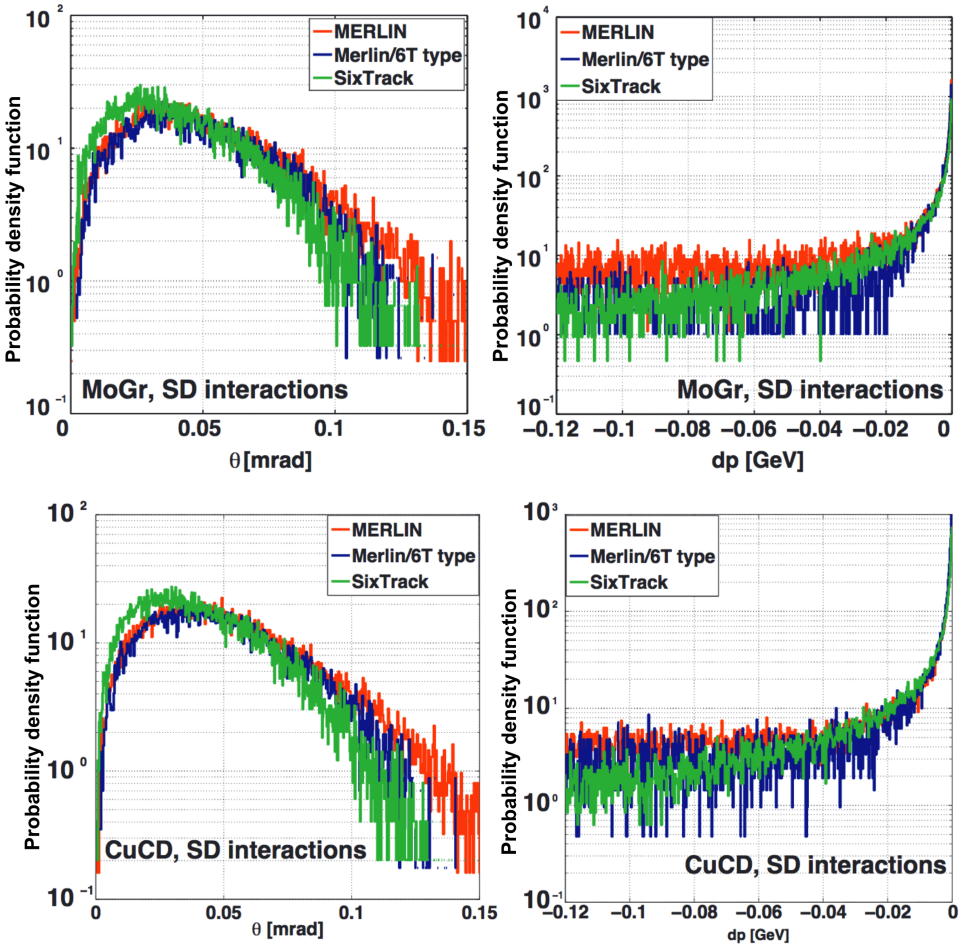

Fig. 2: Distribution of polar angle θ (left) and energy loss dp (right) for single diffractive events in MoGr (top) and CuCD (bottom) block. Comparison of simulation results using "MERLIN-method", "MERLIN-6T-method" and SixTrack.

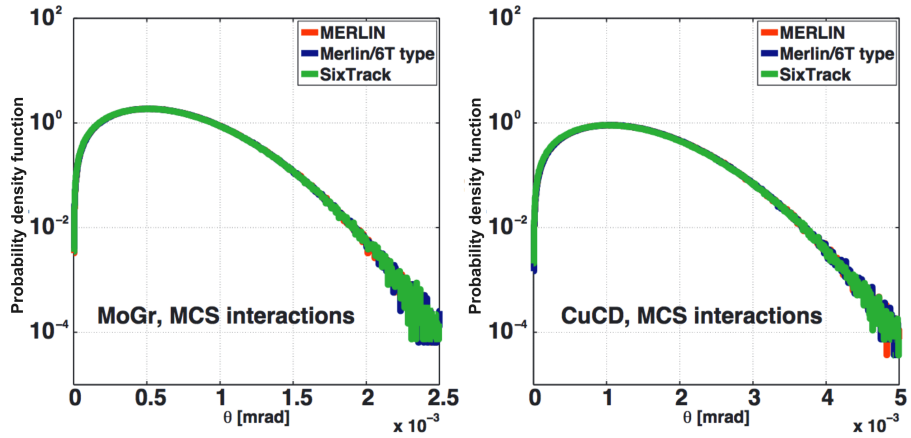

Fig. 3: Distribution of polar angle θ for multiple Coulomb scattering and ionisation events in MoGr (left) and CuCD (right) block. Comparison of simulation results using "MERLIN-method", "MERLIN-6T-method".

5 Evaluation of cleaning performance with advanced collimator materials

The LHC collimation system has to fulfil a number of different functions, such as the beam cleaning functionality [1, 21]: the system must efficiently intercept the unavoidable losses due to the continuous

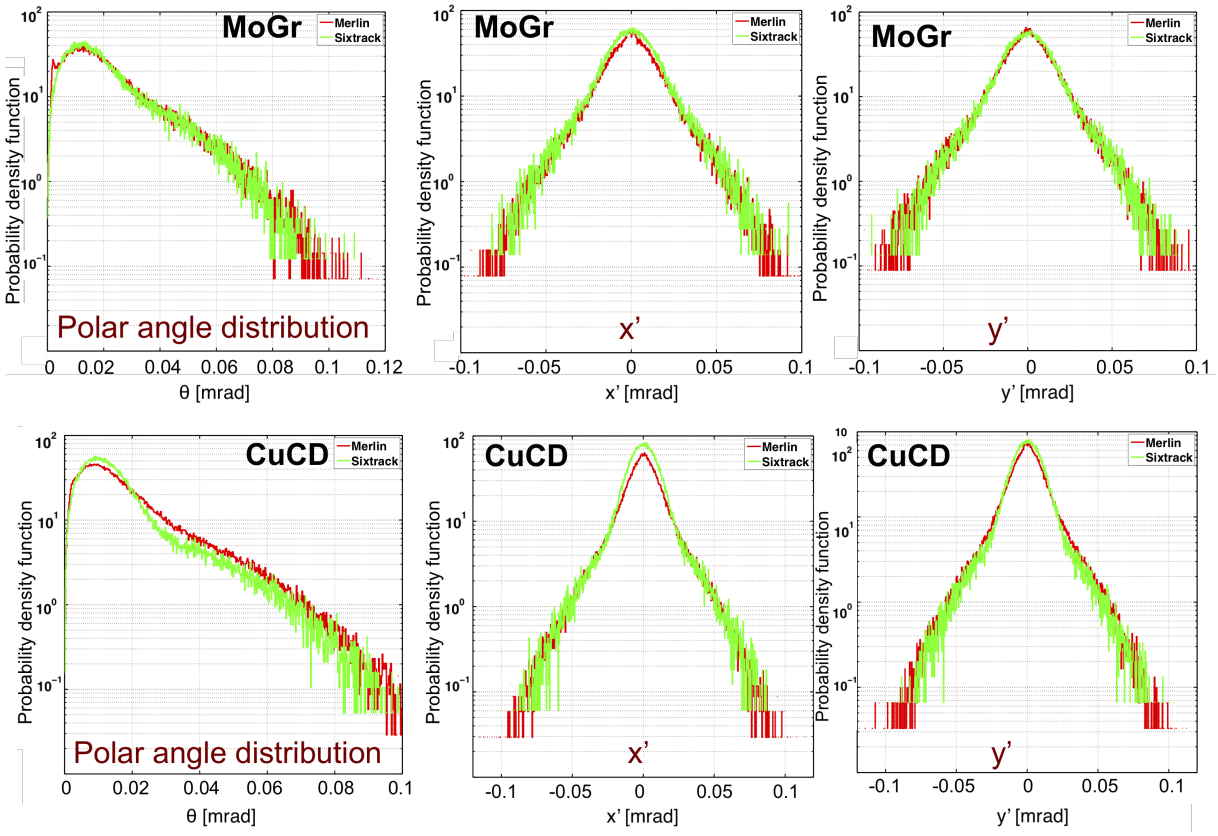

Fig. 4: Polar angle distribution (left) and distributions in x' (center) and y' (right) after 1 cm of CuCD (bottom) and in 1 cm of MoGr (up) of total elastic scattering, comparing MERLIN and SixTrack.

repopulation of the beam halo. The *Local Cleaning Inefficiency* η is used to know the distribution of the losses along the ring and it is expressed by:

$$\eta = \frac{N_{loss}}{\Delta s \cdot N_{abs}} \tag{14}$$

where N_{loss} is the number of particles lost in a Δs length and N_{abs} is the total number of particles absorbed in the collimation system.

In this paper, the effect of new collimator materials on the cleaning efficiency of the LHC collimation system was studied in SixTrack and MERLIN. Tracking simulations were performed for the two beams and in the two planes of halo distribution. The case of the nominal LHC machine at 7 TeV with optics squeezed to $\beta^* = 55$ cm was simulated[1]. In simulations, the full collimation system was in place and the collimator openings were set according to Table 2: a $1\,\sigma$ retraction between primary and secondary collimators in the betratron collimation region IR7 was used, where σ is the local betatronic beam size at the collimator assuming a nominal normalized emittance of 3.5 μm and the design β-function. Same optics parameters, collimator setting and particle statistics were used in both codes to allow a direct comparison of the results.

As of major concern for impedance, IR7 secondary collimators (TCSG) made of CFC were replaced in simulations with new collimator jaws in either MoGr or CuCD. The material implementation described in Section 2 was used in SixTrack, while the equivalent "MERLIN-6T-method" was adopted in MERLIN. In simulations, three cases were considered:

[1]The machine optics is typically adjusted to have a local minimum at the interaction points (experiments), in order to minimize the beam size and thus maximise the interaction rate. The value of the beta function at the interaction points is therefore called β^*.

Table 2: Collimator settings used for in simulation. The values are expressed in units of standard deviation of the beam, calculated for a normalized emittance of 3.5 μm rad. Note that TCL (Target Collimator Long) are located downstream of the secondary collimators (TCSG) in the collimation insertions IR3 and IR7, TCDQ (Target Collimator Dump Quadruple) protect the beam dump line in IR6, and TCT (Target Collimator Tertiary) provide local protection around the interaction points (IP1/2/5/8).

Region	**Collimator Families**	**Settings** [σ]
IR7	TCP / TCSG / TCLA	6 / 7 / 10
IR3	TCP / TCSG / TCLA	15 / 18 / 20
IR6	TCSG / TCDQ	7.5 / 8
IP1/5	TCTs	8.3
IP2/8	TCTs	25

Case 1 (reference) : all IR7 secondary collimators in CFC,

Case 2 : all IR7 secondary collimators in MoGr,

Case 3 : all IR7 secondary collimators in CuCD.

Results obtained with both simulation tools indicate that the losses in the cold dispersion suppressors magnets downstream of IR7, which represent the location of highest losses along the ring for the present system and therefore the main limitation to the cleaning efficiency, are essentially not affected by changing the material of the TCSGs [20, 22]. This result was expected since these losses are dominated by single diffractive events taking place in the upstream primary collimators [23] that are unchanged in these studies. As an example, Fig. 5 shows loss patterns in terms if cleaning inefficiency η simulated by SixTrack in the full LHC and around the IR7 region, compared in the case of CFC (Case 1) and CuCD (Case 3) secondary collimators.

We focus the following analysis on the loss distribution on the IR7 TCSGs, comparing the results obtained by the two codes. The losses on all secondary collimators, expressed in terms of number of the inelastic interactions occurring in the jaw volume, collimator by collimator, are depicted in Fig. 6 for the Case 1-2-3: on the left hand side, the results from SixTrack simulations, and on the right hand side those from MERLIN. Both codes show that the first two TCSG downstream of the primary collimators are progressively more loaded as the effective Z of the composites increases. These collimators intercept the products of the scattering with the primary collimators, and a larger Z values have a direct impact on the effectiveness of the particle absorption. The loss ratio calculated collimator by collimator for the novel composite materials over the present CFC (Fig. 7) shows a loss increase of about 10% for MoGr and 13-18% for CuCD. Differences in losses in the TCSGs further downstream are less apparent and, if any, indicate lower load for the new materials than for the present CFC. This is mainly caused by a larger fraction of secondary halo that is already absorbed by the first two TCSG.

The distribution of the particles lost along the length of the two jaws of the most loaded secondary collimator (TCSG.B5L7) is plotted in Fig. 8: as expected, it shows an exponential decrease due to inelastic scattering events along the jaw length and the slope looks steeper for CuCD and MoGr, materials with higher density and therefore shorter inelastic length, than the case of CFC.

Finally, it is important to stress that the number of destructive interactions of primary protons is not the dominant factor to understand beam losses on a collimator. The energy lost by ionization during the trajectory in the material and the generation of secondary particle shower from nuclear inelastic interactions contribute for the largest part to the total energy deposited in the collimator. Therefore, results of tracking simulations must be complemented by energy deposition and thermo-mechanical studies to have a more complete picture of the effect of beam losses on a beam-intercepting device. Simulations of energy density and mechanical response on new secondary collimators are being performed to confirm that the structural integrity of the composite material jaws will not be compromised by the increased

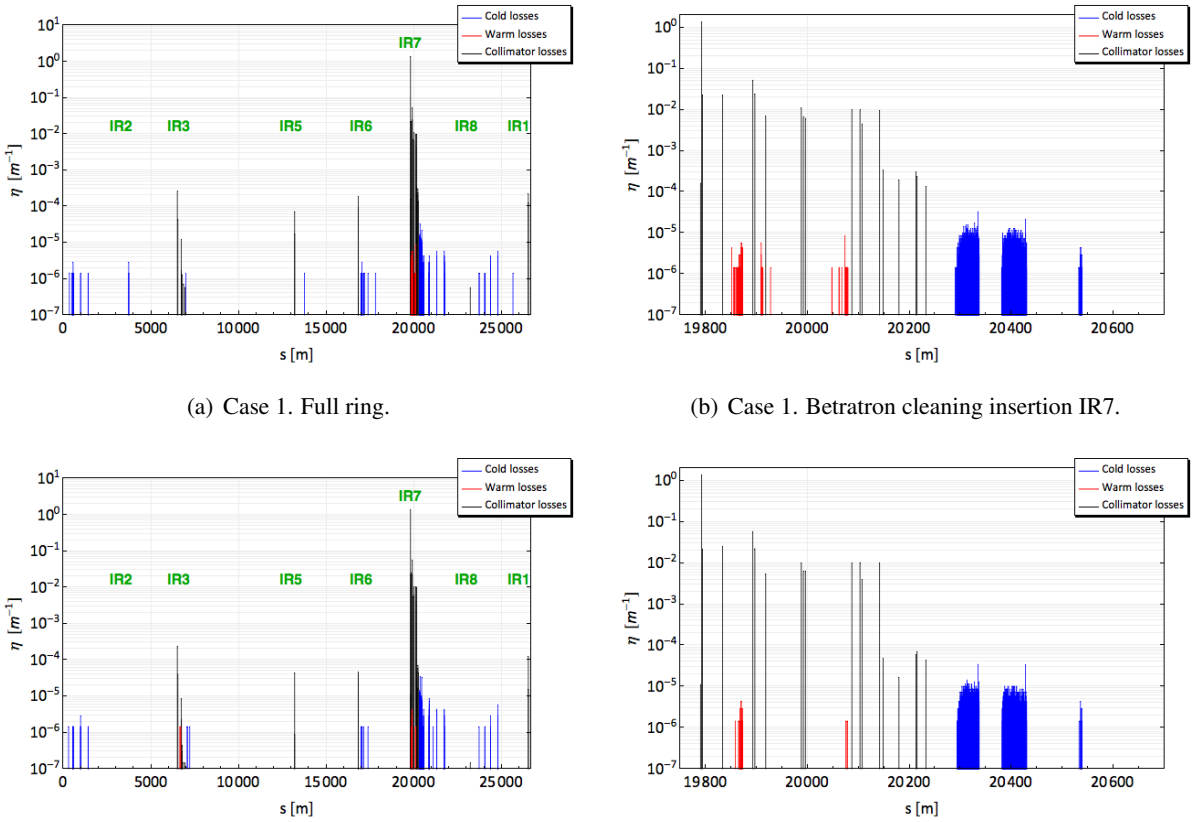

(a) Case 1. Full ring.

(b) Case 1. Betratron cleaning insertion IR7.

(c) Case 3. Full ring.

(d) Case 3. Betratron cleaning insertion IR7.

Fig. 5: Beam loss patterns at 7 TeV in the nominal LHC machine for Beam 1 horizontal halo, simulated by SixTrack. In blue, the losses in the superconductive magnets (cold losses), in red those in the normal-conductive magnets (warm losses) and in black the losses in the collimators.

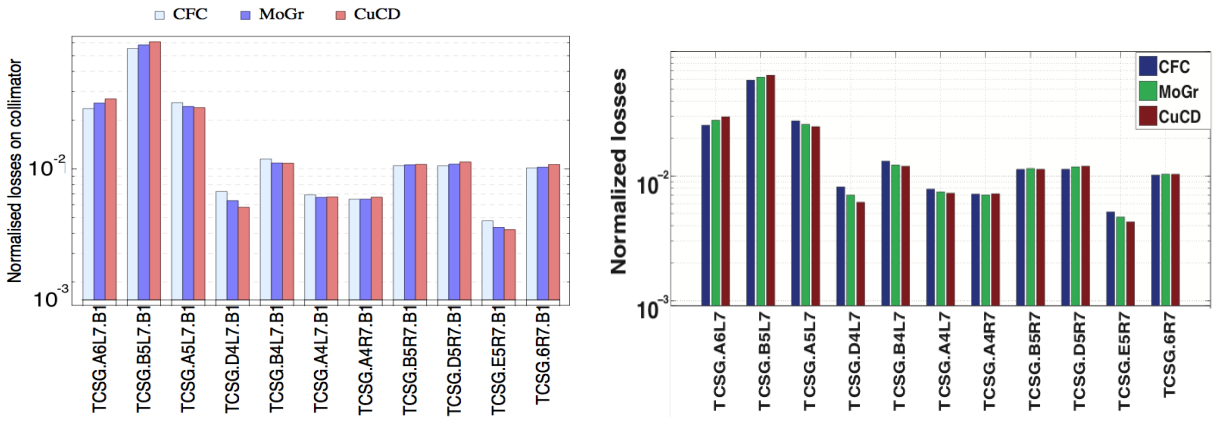

(a) SixTrack simulations.

(b) MERLIN simulations.

Fig. 6: Normalized losses on secondary collimators in IR 7 for different jaw materials, i.e. CFC, MoGr, CuCD, as estimated by SixTrack (left) and MERLIN (right).

energy deposited when denser materials than CFC are used.

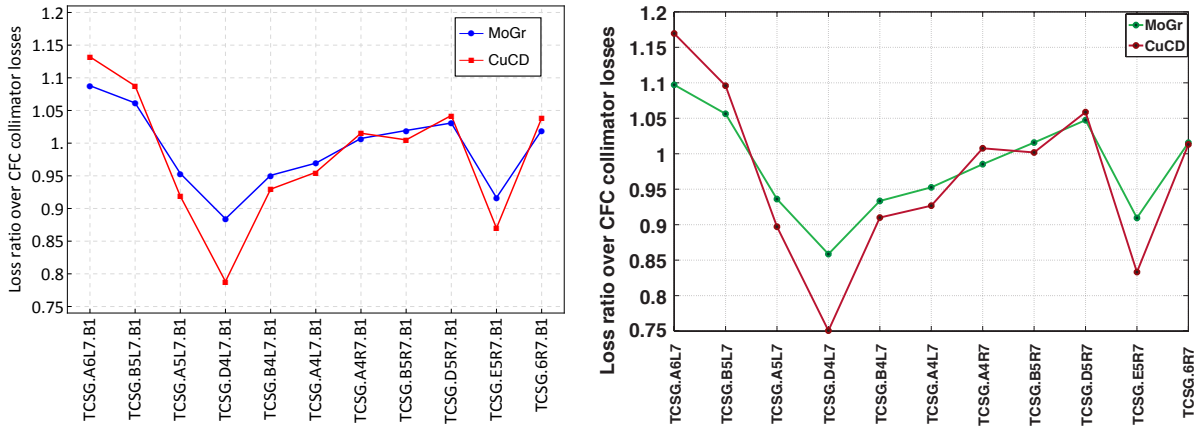

(a) SixTrack simulations. (b) MERLIN simulations.

Fig. 7: Ratio between simulated losses on secondary collimators in IR7 for different jaw materials over the CFC ones, as estimated by SixTrack (left) and MERLIN (right).

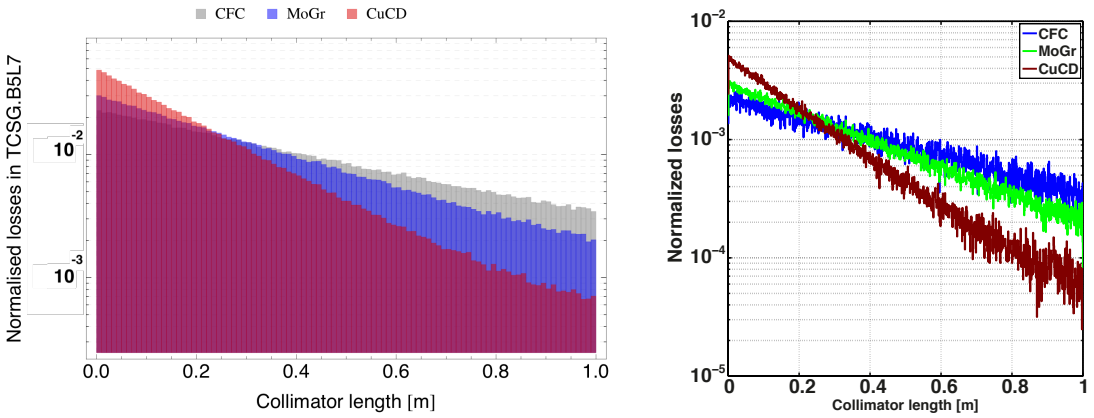

(a) SixTrack simulations. (b) MERLIN simulations.

Fig. 8: Distribution of particles lost along the length of the most loaded TCSG for different jaw materials, as estimated by SixTrack (left) and MERLIN (right).

6 Conclusions and outlook

The need to reduce the impedance contribution of the LHC collimation system for future upgrades of the LHC motivated the development of novel composites that combine high-robustness and reduced electrical resistivity. The possibility to simulate proton interactions with composite materials has been successfully implemented in SixTrack and MERLIN, and is now available for simulations of beam collimation cleaning in the LHC. The SixTrack implementation relies on the calculation of effective material properties, such as cross sections of nuclear events and radiation length, as for a "composite" nucleus. The same approach was tested in MERLIN, which treats composite materials in a different way. From a first comparison of the results obtained with the codes, no relevant differences between the two approaches have been observed. This is an important validation of the newly proposed approach. However, further comparison with other tools, e.g. FLUKA [24,25] and GEANT [26], are planned to be performed in the future.

In this work, we also presented results of halo cleaning studies in the LHC with new collimator materials. Simulations were performed in the same conditions with SixTrack and MERLIN to allow a consistent comparison of the results. Advanced collimators, based on novel low-resistivity composite

materials, were used in simulation to replace present non-metallic secondary collimators. Simulation with both codes confirmed that the cleaning efficiency is only slightly improved when new secondary collimators are used. The outcome was not unexpected, as the main goal of this part of the upgrade was indeed the reduction of the electrical impedance. However, a major improvement of the cleaning performance can be achieved if primary collimators are replaced by a denser jaw material, as discussed in Ref. [27,28], or losses in the dispersion suppressor are locally cleaned [28–30]. The results of cleaning simulations with the full collimation layout are overall consistent with the expectations and this enforces further the validity of the new implementation for the treatment of composite materials.

References

[1] O. Bruning *et al.* (eds), LHC Design Report, Technical report, CERN, Geneva, Switzerland, Rep. CERN-2004-003-V-1, 2004.

[2] R.W. Assmann *et al.*, The final collimation system for the LHC, in: Proceedings of EPAC06, Edimburgh, Ireland, 2006.

[3] N. Mounet *et al.*, Collimator impedance measurements in the LHC, in: Proceedings of IPAC13, Shangai, China, 2013.

[4] I. Bejar Alonso *et al.*, HiLumi LHC Technical Design Report, Technical report, CERN-ACC-2015-0140, 2015.

[5] A. Bertarelli *et al.*, Novel materials for collimators at LHC and its upgrades, in: Proceedings of HB2014, East Lansing, Michigan, 2014.

[6] N. Mariani, Development of novel advanced Molybdenum-based composites for high energy physics applications, Ph.D. thesis, Politecnico di Milano, 2014.

[7] F. Schmidt, SIXTRACK version 1.2: user's reference manual, *CERN/SL/94-56-AP*, 1994.

[8] Sixtrack, `http://sixtrack.web.cern.ch/SixTrack/`.

[9] R. De Maria *et al.*, Recent Developments and Future Plans for SixTrack, in: Proceedings of IPAC13, Shangai, China, 2013.

[10] G. Robert-Demolaize *et al.*, A new version of sixtrack with collimation and aperture interface, *PAC05, Knoxville, USA*, 2005.

[11] C. Tambasco, An improved scattering routine for collimation tracking studies at LHC, Master's thesis, Università La Sapienza, Roma, Italy, 2014.

[12] Merlin, `https://github.com/MERLIN-Collaboration/MERLIN`.

[13] Linear Collider Collaboration, International Linear Collider, `https://www.linearcollider.org/ILC`.

[14] J. Molson, Proton scattering and collimation for the LHC and LHC lumi nosity upgrade., Ph.D. thesis, University of Manchester, 2014.

[15] K. Nakamura *et al.*, Passage of particles through matter, *JPG 37, 075021*, 2010.

[16] K.A. Olive *et al.*, Particle Data Group, 2014.

[17] H. A. Bethe, Moliere's theory of multiple scattering, *Physical Review*, 89, pages 1256–1266, 1953.

[18] A.N. Kalinovskii *et al.*, Passage of High Energy Particles through Matter, AIP-Press, 1898.

[19] A. Mereghetti *et al.*, SixTrack for Clening Studies: 2017 Update, in: IPAC17, Copenhagen, Denmark, 2017.

[20] A. Valloni *et al.*, MERLIN cleaning studies with advanced collimator materials for HL-LHC, in: Proceedings of IPAC16, Busan, South Korea, 2016.

[21] S. Redaelli, R.W.Assmann, G. Robert-Demolaize, LHC aperture and commissioning of the collimation system, pages 268–277, 2005.

[22] E. Quaranta *et al.*, Collimation cleaning at the LHC with advanced secondary collimator materials,

in: Proceedings of IPAC15, Richmond, Virginia, 2015.

[23] C. Bracco, Commissioning Scenarios and Tests for the LHC Collimation System, Ph.D. thesis, EPFL Lausanne, 2008.

[24] A. Ferrari *et al.*, FLUKA : A multi-particle transport code (program version 2005), *CERN-2005-010*, 2005.

[25] T.T. Bohlen *et al.*, The FLUKA code: Developments and challenges for high energy and medical applications, *Nuclear Data Sheets*, (120), pages 211–214, 2014.

[26] Geant4, `https://geant4.web.cern.ch/geant4`.

[27] A. Valloni *et al.*, Comparison between different composite material implementations in Merlin, Presentation at the 71st Collimation Upgrade Specification Meeting, CERN, May 23rd, 2016.

[28] E. Quaranta, Investigation of collimator materials for the High Luminosity Large Hadron Collider, Ph.D. thesis, Politecnico di Milano, Italy, 2017 (to be published).

[29] E. Quaranta *et al.*, Towards optimum material choices for HL-LHC collimation upgrade, in: Proceedings of IPAC16, Busan, South Korea, 2016.

[30] D. Mirarchi *et al.*, Cleaning performance of the collimation system of the High Luminosity Large Hadron Collider, in: Proceedings of IPAC16, Busan, South Korea, 2016.